Supporting Information

In-situ Growth of ZnO Nanostructures on the Pores and Surface of Soft 3D Structures for Energy Storing, Conversion and Bioinspired Sensing

*Jithin Kanathedath[1], Febin Paul[1], Anuja Sasi[2], Anitta Mathew[2], Mustehsan Beg[1], Diana Gaspar[2,3], Nazmi Sellami[1], Firdaus Muhammad-Sukki[1], Luis Pereira[2,3], Libu Manjakkal[1]**

[1]School of Computing, Engineering & the Built Environment, Edinburgh Napier University, Merchiston Campus, EH10 5DT, UK.

[2]CENIMAT/i3N, Department of Materials Science, NOVA School of Science and Technology NOVA University Lisbon (FCT-NOVA) and CEMOP/UNINOVA Campus de Caparica, Caparica, 2829-516, Portugal

[3]AlmaScience Colab, Madan Parque, 2829-516 Caparica, Portugal

Table ST1. Comparison of reported works on multifunctional devices

No.	Materials	Functions	Energy storage performance	Sensing performance	Energy conversion	References
1	PDMS foam/MWCNT/ZnO flexible electrode device	Energy storage, Capacitive pressure sensing and Energy conversion	Specific capacitance: 0.57 F g^{-1} at 2.1 mA g^{-1};	Sensitivity: 2.95 %/kPa; Response time: ~1 s, Recovery time: 2.8 s	Current ~2 mA at 39.2 kPa	This Work
2	Flexible piezoelectric nanogenerator as a self-charging supercapacitor device	Energy storage and energy conversion	Specific capacitance: 21 F g^{-1} at 5 mV s^{-1}	-	Current ~ 1.1 µA at 49 kPa	[1]
3	PPy/ATA	Energy storage and pressure sensing	Specific capacitance: 345.7 mF/cm^2 @ 0.5 mA/cm^2	Sensitivity: 0.841/kPa, response: 0.15s	-	[2]
4	Zn–Co MOFs@MXene	Energy storage and strain sensing	144.7 F/g @ 1 A/g	sensitivity 1.52 GF (0–400%)	-	[3]
5	ZnO/f-MWCNT	Energy storage and Piezoelectric generation	794 F/g at 1 A/g	-	80 V open circuit voltage	[4]

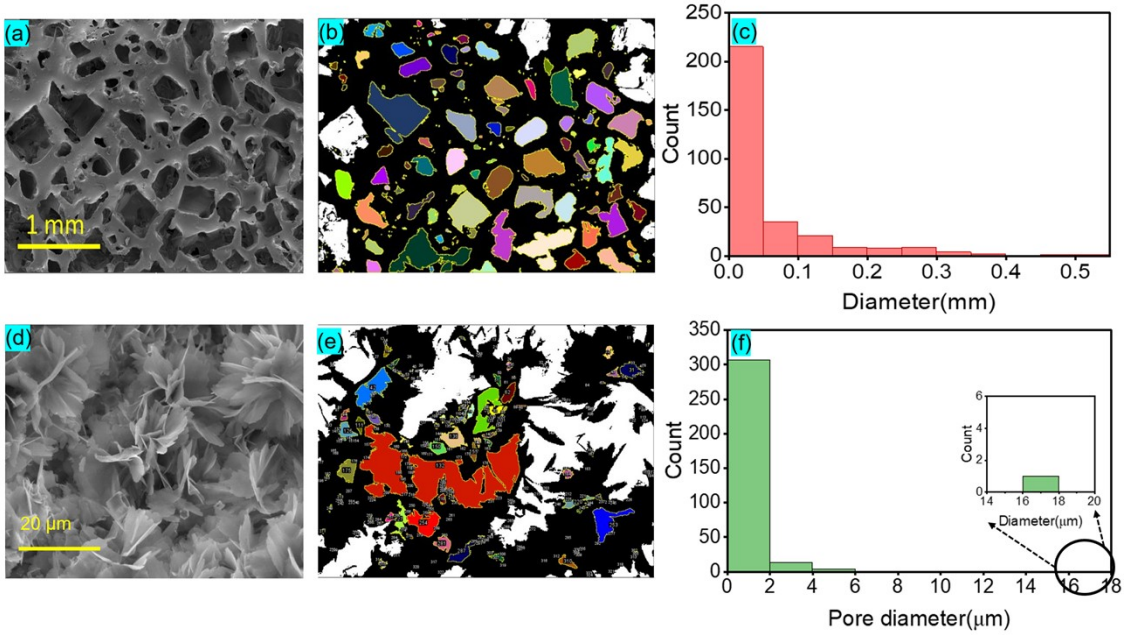

Figure S1 (a), (b) and (c) SEM image, no. of pores and pore size distribution of PDMS foam respectively (d), (e) and (f) SEM image, no. of pores and pore size distribution of PDMS foam after ZnO growth respectively

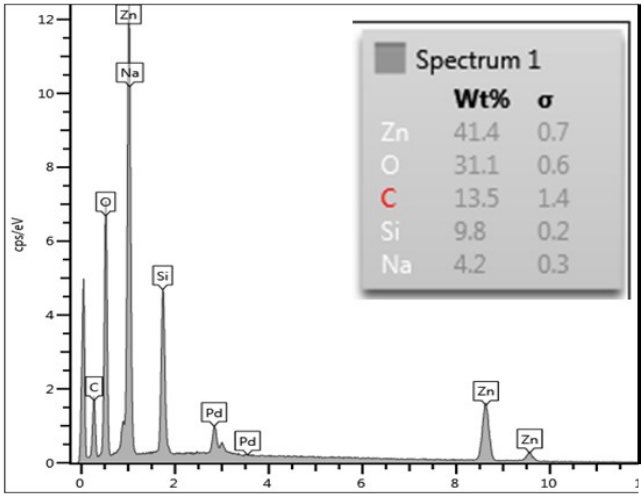

Figure S2. EDX Analysis of PDMS/MWCNT/ZnO

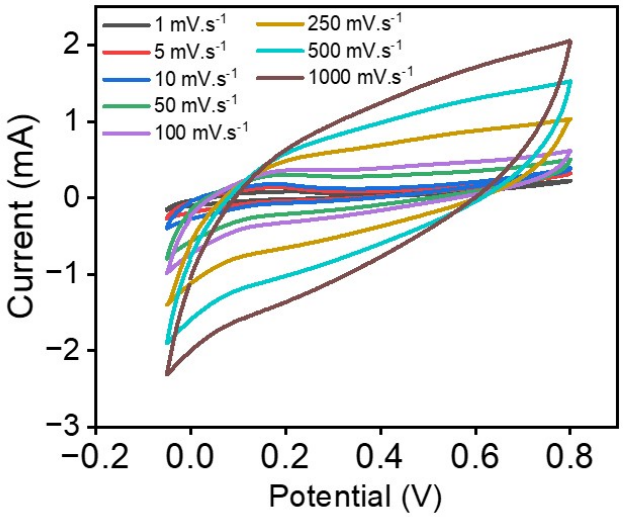

Figure S3. CV Curve at different scan rates using KOH electrolyte without external pressure

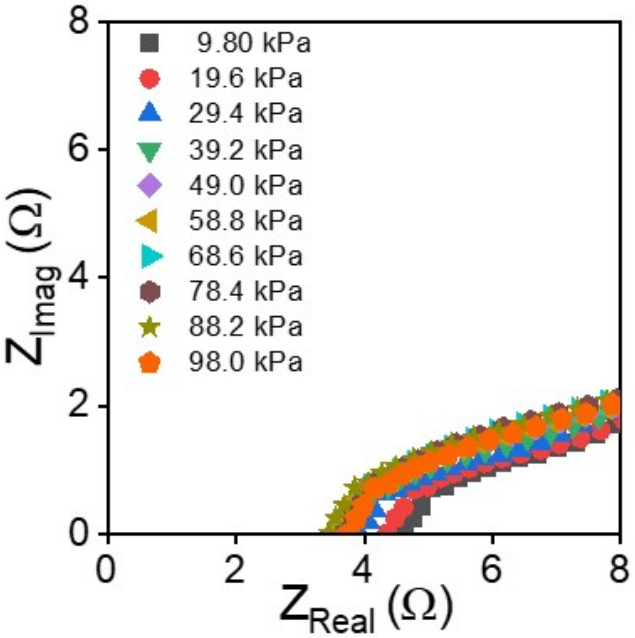

Figure S4. Variation of solution resistance with pressure using KOH electrolyte

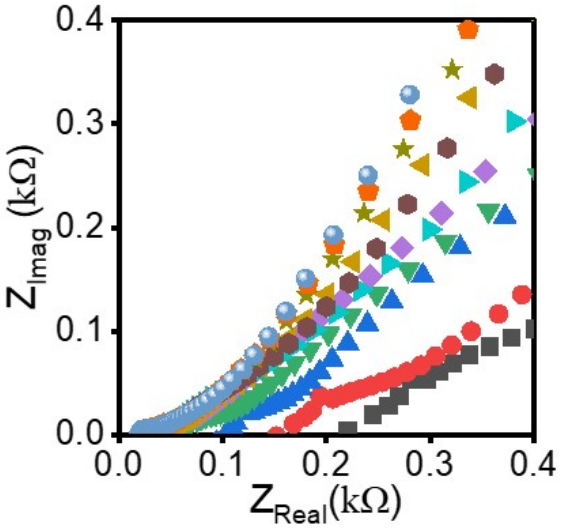

Figure S5. Variation of solution resistance with pressure using NaCl gel electrolyte

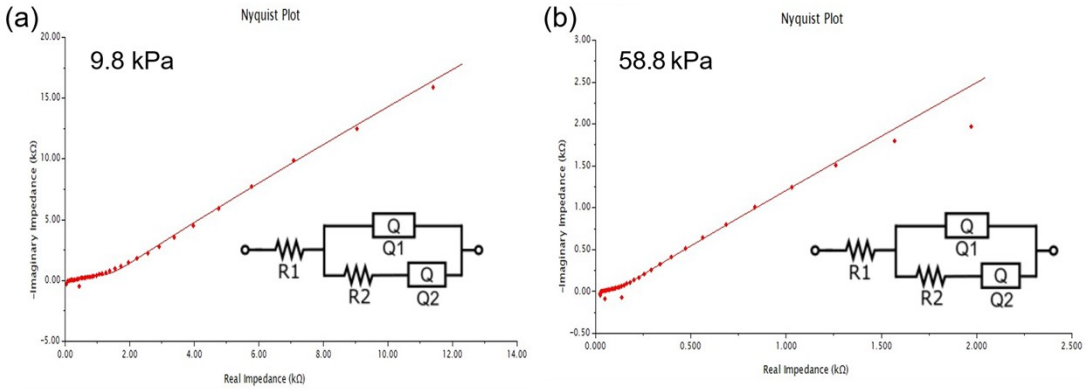

(c)

Components	Value	
	9.8 kPa	**58.8 kPa**
R1	289.33 Ω	52.36 Ω
Q1	76.97 μs°/Ω	922.20 μs°/Ω
R2	1645.74 Ω	244.77 Ω
Q2	211.53 μs°/Ω	0.672 μs°/Ω

Figure S6 (a) and (b) EIS fitting of the PDMS/MWCNT/ZnO device with NaCl-PVA electrolyte at an applied pressure of 9.8 kPa and 58.8 kPa respectively (c) comparison table of fitted components values

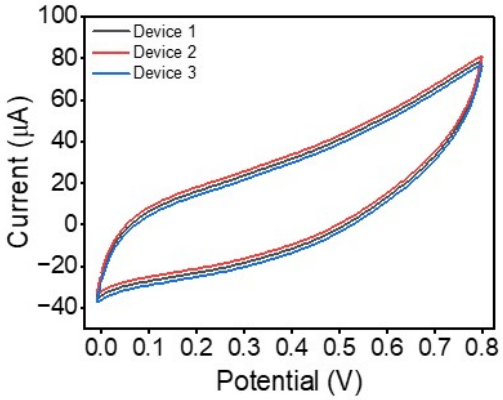

Figure S7. CV curves showing the repeatability of the device under the same applied pressure (9.8 kPa)

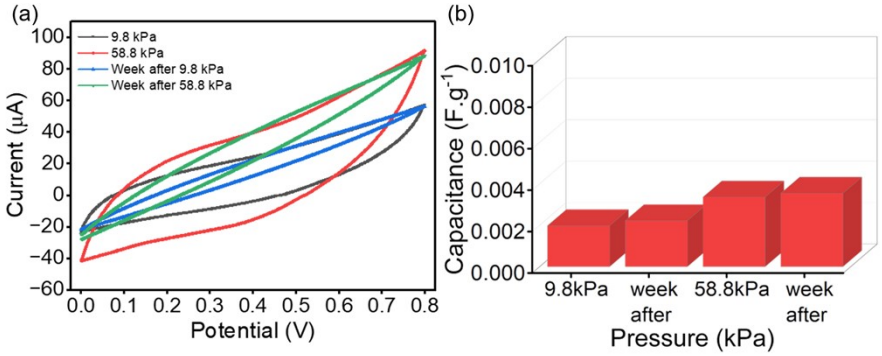

Figure S8. (a) Comparison of CV curves at two different applied pressure before and after a week (b) Capacitance at two different applied pressure before and after a week

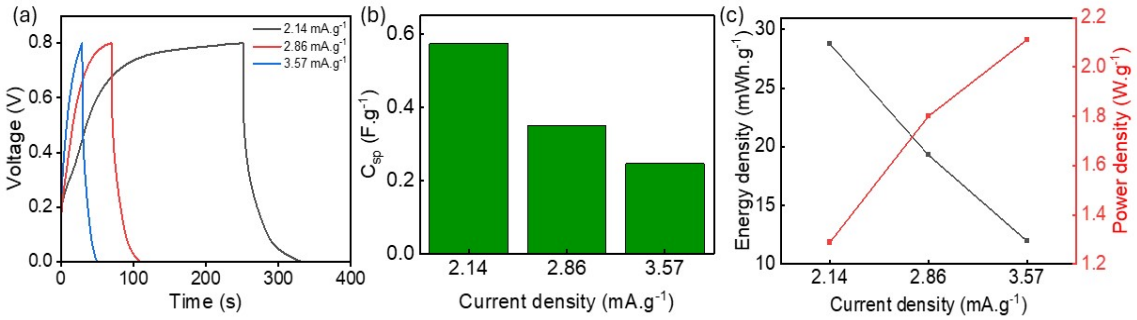

Figure S9. (a) GCD curve at various current densities using KOH electrolyte (b) Specific capacitance at different current densities (c) Energy and power density at different current densities

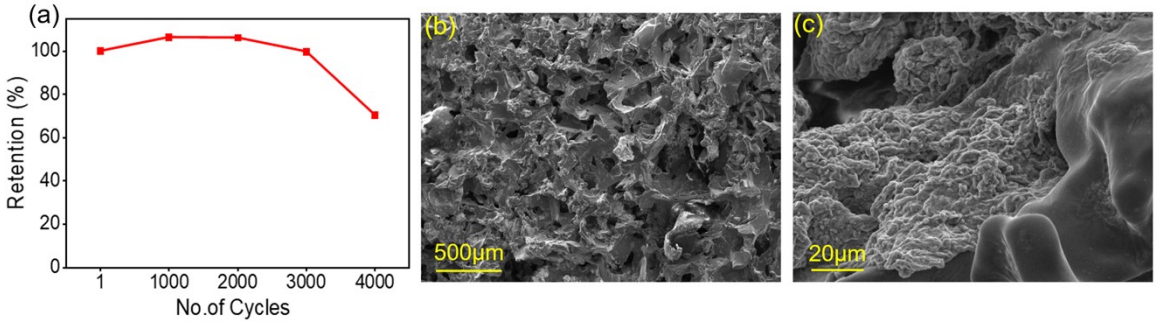

Figure S10. (a) Capacitive retention of device over 4000 charge-discharge cycles (b) and (c) SEM image of the postmortem device after the long cycling at the magnification of 500µm and 20µm respectively

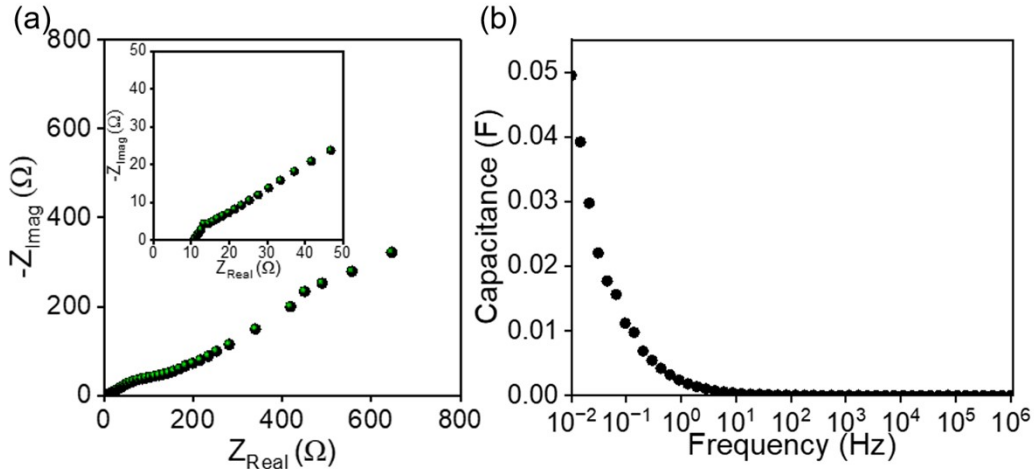

Figure S11 (a) Nyquist plot of the device with KOH electrolyte without external force (b)Variation of Capacitance with frequency

The graph illustrates the frequency dependence of capacitance, showing a marked decline as frequency increases. At low frequencies, the capacitance is relatively high, reaching values near 0.05 F at 10 mHz. This behavior reflects the ability of charge carriers to follow the slowly varying electric field, producing strong polarization effects. As the frequency rises, capacitance decreases sharply, and by the 10 Hz range and beyond it approaches zero. This indicates that the system's capacity to store charge diminishes because charge carriers can no longer keep up with the rapidly oscillating field.

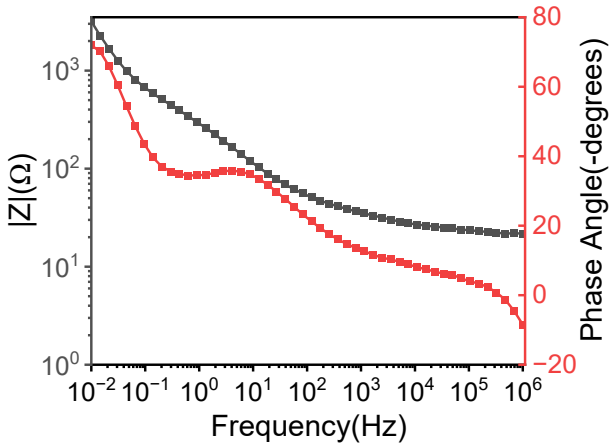

Figure S12. Bode plot of the device PDMS/MWCNT/ZnO

Bode plot represents the Bode magnitude and Bode phase angle graphs, which are shown in the supporting information Figure S7. At low frequencies, the impedance magnitude is at its highest, indicating significant resistance to ion transport within the electrode matrix. As the frequency increases, impedance decreases sharply, signifying enhanced charge transfer kinetics and reduced ion diffusion limitations. Similarly, at low frequencies, the phase angle approaches approximately 80°, characteristic of dominant capacitive behaviour, which reflects strong double-layer capacitance and effective ion accumulation at the electrode–electrolyte interface. With increasing frequency, the phase angle gradually decreases toward zero, indicating a transition from capacitive to resistive behaviour.

Table ST2. Comparison of reported work on PDMS/CNT pressure sensor

Work	**Dielectric / Structural Design**	**Sensitivity (kPa^{-1})**	**Pressure Range**	**Ref.**
CNT/PDMS spinosum-templated sensor	Bio-inspired spinosum CNT/PDMS dielectric	~0.25	0–500 kPa	[5]
Screen-printed CNT/PDMS sensor	CNT/PDMS composite with printed electrodes	~2.9	0–0.45 kPa	[6]
CNT/PDMS multiloading sensor	CNT-filled PDMS dielectric layer	2.90 (<0.45 kPa) 1.87 (0.45–0.85 kPa)	<1 kPa	[7]
MWCNT/TIO_2/PDMS hemispherical sensor	Micro-hemispherical PDMS with MWCNT/TiO_2 fillers	1.89–7.08	0–95 kPa	[8]
Porous MWCNT/PDMS sensor	Porous CNT/PDMS dielectric layer	~2.42	Low-pressure regime	[9]
PDMS/MWCNT/ZnO	In-situ hydrothermal ZnO growth on PDMS/MWCNT	2.95	9.8-98.9 kPa	This work

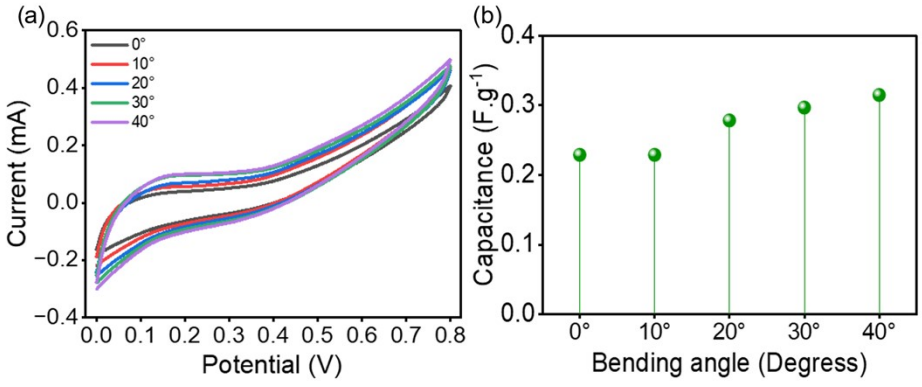

Figure S13 PDMS PDMS/MWCNT/ZnO device with KOH electrolyte (a) CV at different bending angle (b) bending angle vs capacitance

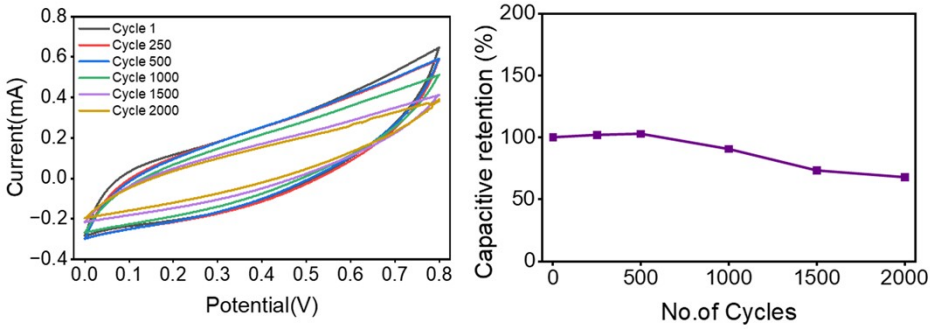

Figure S14 (a) 2000 CV Cycle test of bending device at 100 $mV.s^{-1}$ under the bending angle of 30 degrees (b) capacitive retention

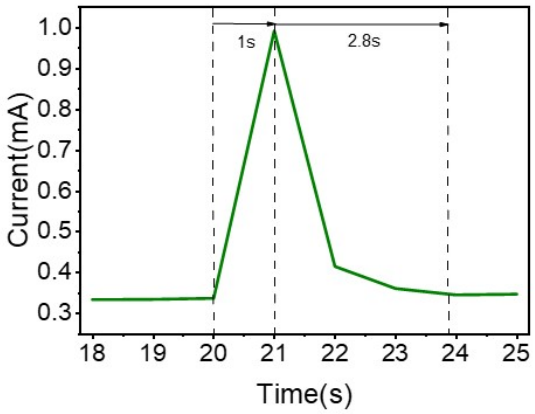

Figure S15: Response and recovery time of the device

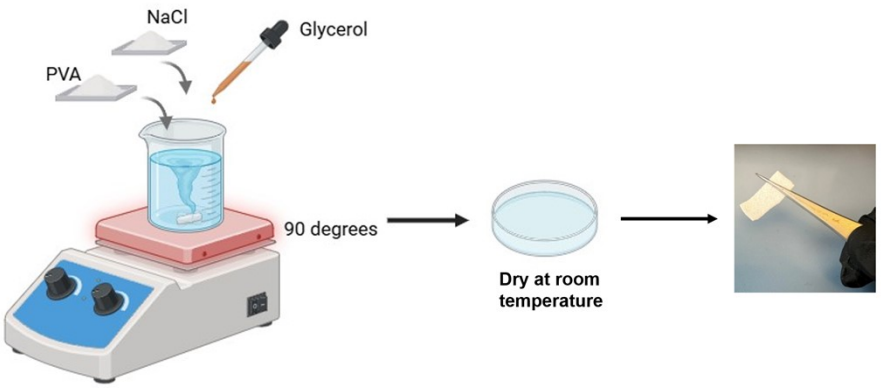

Figure S16. Preparation of NaCl gel electrolyte

References

[1] T. Das, S. Tripathy, A. Kumar, and M. Kar, "Flexible piezoelectric nanogenerator as a self-charging piezo-supercapacitor for energy harvesting and storage application," *Nano Energy,* vol. 136, p. 110752, 2025/04/01/ 2025, doi: https://doi.org/10.1016/j.nanoen.2025.110752.

[2] L. Zhou, Q. Xin, J. Lin, S. Liang, and G. Yang, "A low-cost hydrogel with high conductivity and flexibility for pressure sensor and supercapacitor," *Applied*

Materials Today, vol. 34, p. 101907, 2023/10/01/ 2023, doi: https://doi.org/10.1016/j.apmt.2023.101907.

[3] G.-T. Xiang *et al.*, "Flexible solid-state Zn-Co MOFs@MXene supercapacitors and organic ion hydrogel sensors for self-powered smart sensing applications," *Nano Energy,* vol. 118, p. 108936, 2023/12/15/ 2023, doi: https://doi.org/10.1016/j.nanoen.2023.108936.

[4] A. Baral, N. Bose, B. Show, N. R. Bandyopadhyay, and N. Mukherjee, "ZnO/f-MWCNT as a potential candidate for supercapacitive energy storage and piezoelectric energy generation," *Materials Today Chemistry,* vol. 31, p. 101627, 2023/07/01/ 2023, doi: https://doi.org/10.1016/j.mtchem.2023.101627.

[5] S. Masihi *et al.*, "Highly sensitive porous PDMS-based capacitive pressure sensors fabricated on fabric platform for wearable applications," *ACS sensors,* vol. 6, no. 3, pp. 938–949, 2021.

[6] X. Riedl, C. Bolzmacher, R. Wagner, K. Bauer, and N. Schwesinger, "A novel PDMS based capacitive pressure sensor," in *SENSORS, 2010 IEEE*, 2010: IEEE, pp. 2255–2258.

[7] D. Guo *et al.*, "Highly flexible and sensitive pressure sensor: fabrication of porous PDMS/Graphene composite via laser thermoforming," *Advanced Sensor Research,* vol. 3, no. 5, p. 2300165, 2024.

[8] Y. Ouyang, J. Lei, S. Li, G. He, and S. He, "Highly Sensitive Capacitive Pressure Sensor Based on MWCNTs/TiO2/PDMS with a Microhemispherical Array and APTES-Modified Interface," *Polymers,* vol. 18, no. 1, p. 12, 2025.

[9] A. H. Chowdhury, B. Jafarizadeh, N. Pala, and C. Wang, "Wearable capacitive pressure sensor for contact and non-contact sensing and pulse waveform monitoring," *Molecules,* vol. 27, no. 20, p. 6872, 2022.